

# Synthesis of copolymer electrolytes based on polysiloxane and their high temperature durability analysis for solvent-free dye-sensitized solar cells

Fu-Ming Wang · Chia-Hsien Chu · Yung-Liang Tung ·  
Bing-Joe Hwang · Yung-Yun Wang · Chi-Chao Wan ·  
Raman Santhanam

Received: 14 January 2011 / Revised: 7 April 2011 / Accepted: 11 April 2011 / Published online: 4 May 2011  
© Springer-Verlag 2011

**Abstract** The present work develops a new type of solvent-free copolymer electrolyte based on polysiloxane for dye-sensitized solar cells (DSSCs). The electrolyte is characterized by conductivity measurements, hydrogen-1 nuclear magnetic resonance spectroscopy, rheology, and DSSC performance. Repeated units of the ethylene oxide on methylhydrosiloxane show plasticizing effects and enhanced durability of the

DSSCs. DSSC employing the polysiloxane electrolytes show no energy conversion efficiency decay after 16 days test at room temperature and yields a conversion efficiency of 1.5% during long-term stability measurement at 90 °C under white light irradiation of 100 mW cm<sup>-2</sup>. The new solvent-free polysiloxane copolymer electrolyte can be good candidate for next generation DSSC.

F.-M. Wang  
Nanoelectrochemistry Laboratory,  
Graduate Institute of Engineering,  
National Taiwan University of Science and Technology,  
Taipei, Taiwan

F.-M. Wang (✉)  
Sustainable Energy Center,  
National Taiwan University of Science and Technology,  
43 Keelung Road, Section 4,  
Taipei 106, Taiwan  
e-mail: mccabe@mail.ntust.edu.tw

C.-H. Chu · Y.-Y. Wang · C.-C. Wan  
Department of Chemical Engineering,  
National Tsing Hua University,  
Hsinchu, Taiwan

Y.-L. Tung  
Photovoltaics Technology Center,  
Industrial Technology Research Institute,  
Chutung, Hsinchu, Taiwan

B.-J. Hwang  
Nanoelectrochemistry Laboratory,  
Department of Chemical Engineering,  
National Taiwan University of Science and Technology,  
Taipei, Taiwan

R. Santhanam  
Maxwell Technologies,  
San Diego, CA, USA

**Keywords** Siloxane · Solvent free · Polymer electrolyte · Dye-sensitized solar cell

## Introduction

Dye-sensitized solar cells (DSSC) have attracted great attention since the pioneering concept proposed by O'Regan and Gratzel in 1991 in view of their lower cost, easy processing compared to that of silicon-based solar cells [1], and provided appropriate conversion efficiency. The electrolyte generally used in DSSCs is I<sup>-</sup>/I<sup>3-</sup> redox couple in an organic solvent, and it has been reported that DSSCs can give a high conversion efficiency of 10–11% [2]. However, the presence of liquid electrolytes is the key barrier to the commercialization of DSSCs. Liquid electrolytes commonly suffer from liquid volatilization and leakage and thus limit the long-term stability of the DSSCs [3]. Therefore, several approaches have been made to replace liquid electrolytes; and among those approaches, the use of polymer electrolytes appears to deliver high conversion efficiency [4]. For the past decade, poly(ethylene oxide) (PEO) is the most extensively researched topic because of its potential use as solvent-free or gel polymer electrolytes in both lithium-ion batteries [5, 6] and DSSCs [7–10]. However, PEO has poor conductivity ( $\sigma \sim 10^{-7}$  S cm<sup>-1</sup>) due to its high degree of

crystallinity at ambient temperature. Several methods have been developed to improve the ionic conductivity of PEO-based polymer electrolytes. These methods include utilizing metal oxides, such as  $\text{Al}_2\text{O}_3$ ,  $\text{TiO}_2$ , and  $\text{SiO}_2$ , well-mixed with PEO [11–14], as well as atactic poly(propylene oxide) randomly copolymerized with ethylene oxide (EO) [15]. These modifications suppress the vibration of the polymer chains and as a result enhance ionic transfer and prevent the crystallization of the matrix polymers [16]. For example, Singh et al. [17] used the low viscosity ionic liquid EMImTFSI mixed with PEO as the plasticizing effect, which reduces the crystallinity. Optical microscope observation reveals an increase in the amorphous region with the decrease in the size of the spherulites. However, ionic transfer requires a flexible and soft supporting backbone according to the basic principle of electrochemical reactions.

In this regard, polysiloxane has a low glass transition temperature ( $T_g$ ) of  $-123\text{ }^\circ\text{C}$  for poly(dimethylsiloxane) and an extremely high free volume [18], which indicates the excluded volume of a polymer system and the polymer atoms do not take up the space. This can provide an adequate ion-hopping site for the transfer of lithium-ions to the polymer backbone. Wang et al. [19–21] developed a new series of polysiloxane based on polymer electrolytes and studied their properties such as free volume, ionic transfer mechanism, and lithium-ion battery performance. These new polysiloxanes with acrylate-ethylene oxide substituted side chain become a hydrophobic–hydrophilic block polymer that enhances the adhesion.

In this article, the new polysiloxane-based electrolytes are synthesized and their ionic conductivity; polymer rheology and the effects of cell performance on varying repeat units of poly(methylhydrosiloxane) (PMHS); and a typical molecular weight of poly(ethyl glycol) methyl ether methacrylate (PEGMEMA) using hydrosilylation reaction to enhance the durability, long life, and high temperature application in DSSCs were studied.

## Experimental

### Materials

PMHS ( $M_n=390$ , 2,700) and PEGMEMA ( $M_n=475$ ) were purchased from Aldrich and dried prior to use for 72 h using  $4\text{ \AA}$  molecular sieves. Platinum (0)-1,3-divinyl-1,1,3,3-tetramethyldisiloxane Pt (dvs), lithium iodide (LiI), iodine ( $\text{I}_2$ ), ammonium iodide ( $\text{NH}_4\text{I}$ ), tetrabutylammonium iodide (TBAI), 1-propyl-3-methylimidazolium Iodide (PMII), 1-propyl-2,3-dimethylimidazolium iodide (DMPII), and acetonitrile (AN) were also purchased from Aldrich. A 3 wt.% solution of Pt (dvs) in isopropanol was prepared in our laboratory. Nuclear magnetic resonance (NMR)-grade

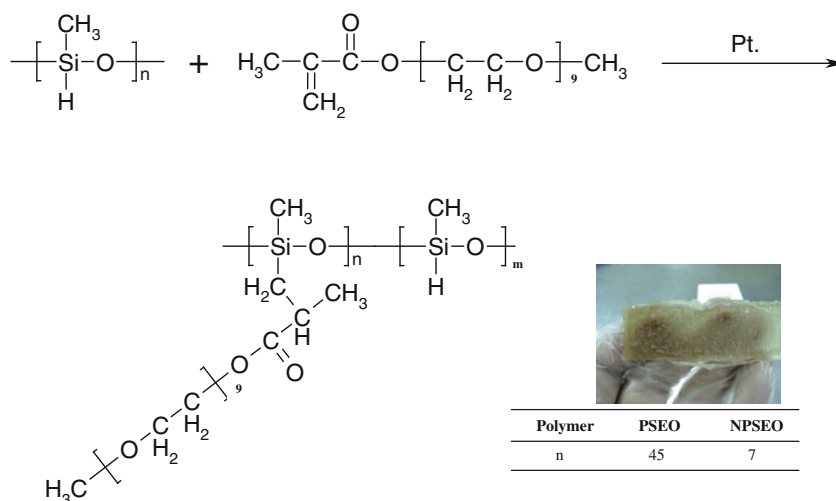
$\text{CDCl}_3$  was stored in a glove box. Twenty nanometer  $\text{TiO}_2$  was purchased from JGC Catalysts and Chemicals Ltd and the  $\text{TiO}_2$  paste was prepared by ITRI.

### Preparation of polysiloxane electrolytes

The hydrosilylation of two PMHSs were carried out using a platinum catalyst and PEGMEMA. Injected into a 250-ml, three-necked round-bottom flask called PSEO were 1.52 g (0.025 mol) of PMHS<sub>2700</sub>, 13.06 g (0.025 mol) of PEGMEMA<sub>475</sub>, and 150 ml of tetrahydrofuran (THF). In the meanwhile, 1.52 g (0.025 mol) of PMHS<sub>390</sub>, 1.94 g (0.025 mol) of PEGMEMA<sub>475</sub>, and 150 ml of THF were also injected into another 250-ml, three-necked round-bottom flask called NPSEO. The molarity ratios of the PEGMEMA and the Si-H group from PMHS were 1:1.05. The resulting colorless homogeneous solution of mixing solvent with PEGMEMA and THF was heated to  $80\text{ }^\circ\text{C}$  under  $\text{N}_2$ . The solution, together with the functionalized polysiloxane precursor and  $90\text{ }\mu\text{l}$  of Pt (dvs), was injected into the reactor. This reaction was maintained for 72 h until almost no residual  $-\text{C}=\text{C}-$  or  $-\text{Si}-\text{H}$  groups were detected in the  $^1\text{H}$ ,  $^{13}\text{C}$ , or  $^{29}\text{Si}$  NMR spectra. The resulting light brown polymer (shown in Scheme 1) was extracted four times with *n*-hexane to remove the catalyst and residual precursors. After purification, the polysiloxane was dissolved in THF and its molecular weight was determined against a polystyrene standard using gel permeation chromatography. The molecular weight of functionalized PSEO and NPSEO were  $1.2 \times 10^5$  and  $3.8 \times 10^4$  ( $\text{mol g}^{-1}$ ), respectively.

The infrared absorbance spectrum indicates a very weak absorption band at  $2,160\text{ cm}^{-1}$ , corresponding to  $\nu$  (Si-H), and a very strong band at  $1,104\text{ cm}^{-1}$ , corresponding to  $\nu$  (Si-O-Si). PSEO exhibits hydrogen-1 nuclear magnetic resonance ( $^1\text{H}$  NMR;  $\text{CDCl}_3$ ) of  $\delta$  (ppm)=4.07, 3.75–3.37, 2.03–1.83, 1.31–0.86, and 0.06;  $^{13}\text{C}$  NMR ( $\text{CDCl}_3$ ) of  $\delta$  (ppm)=177.4, 77.3–76.7, 71.9, 70.6–70.5, 68.5, 67.9, 59.0, 45.0, 29.7, and 25.6; and  $^{29}\text{Si}$  NMR ( $\text{CDCl}_3$ ) of  $\delta$  (ppm)= $-80$  to  $-120$  (broad peak). NPSEO exhibits  $^1\text{H}$  NMR ( $\text{CDCl}_3$ ) of  $\delta$  (ppm)=4.10–4.09, 3.60–3.58, 3.57–3.42, 1.76–1.73, 1.26–1.18, 1.11, and 0.07;  $^{13}\text{C}$  NMR ( $\text{CDCl}_3$ ) of  $\delta$  (ppm)=176.2, 72.3–69.5, 71.9, 67.8, 58.0, 63.4, 39.8 to 39.3, 33.9, 27.4, and 17.9; and  $^{29}\text{Si}$  NMR ( $\text{CDCl}_3$ ) of  $\delta$  (ppm)= $-100$  to  $-120$  (broad peak).

For the solvent-free electrolyte preparation, the PSEO and NPSEO were prepared by mixing 0.5 M  $\text{NH}_4\text{I}$ , 0.1 M TBAI, and 0.5 M DMPII under continuous stirring for 8 h, a THF mixed solvent combined with 0.1 M LiI and 0.2 M  $\text{I}_2$  to prepare the substituted polysiloxane electrolytes for maximizing the dissolution of the salt in THF. The electrolyte solvent was loaded into a Teflon cell consisting of two stainless steel electrodes, which researchers then seal with O-rings. The electrolyte is vacuum-dried at a pressure of less than 1 atm at

**Scheme 1** Synthesis of substituted polysiloxanes and the photograph of PSEO

50 °C for 48 h to remove the THF solvent and prevent the electrolyte from bubbling. This study obtains the ionic conductivity of the highly viscous functionalized polysiloxane electrolytes as a function of temperature using alternating current (AC) impedance. The AN liquid electrolyte was also prepared by mixing the same composition of 0.5 M  $\text{NH}_4\text{I}$ , 0.1 M TBAI and 0.5 M DMPII under continuous stirring for 8 h with  $\Gamma/\Gamma^{3-}$  redox-couple (0.1 M LiI, 0.2 M  $\text{I}_2$ ).

#### Preparation of the nanocrystalline $\text{TiO}_2$ and counter electrode

The fluorine-doped tin oxide (FTO) glass used as current collector was first cleaned in a detergent solution using an ultrasonic bath for 15 min, and then rinsed with water and ethanol [22]. After treatment in a UV- $\text{O}_3$  system (Model No. 256–220, Jelight Company, Inc.) for 18 min, the FTO glass plates were immersed into a 40 mM aqueous  $\text{TiCl}_4$  solution at 70 °C for 30 min and washed with water and ethanol. There are two types of  $\text{TiO}_2$  pastes forming, respectively, the transparent and the light-scattering layers of the photo-anode: nanocrystalline- $\text{TiO}_2$  (20 nm, paste A) and microcrystalline- $\text{TiO}_2$  (400 nm, paste B) particles. A layer of paste A was coated on the FTO glass plates by screen-printing (90 T, EstalMono, Schweiz. Seidengazefabrik, AG, Thal), kept in a clean box for 3 min so that the paste microstructure could readjust to reduce the surface irregularity and then thus dried for 6 min at 125 °C. After drying at 125 °C, two layers of paste B were deposited by screen printing, resulting in a light-scattering  $\text{TiO}_2$  film containing 400-nm sized anatase particles of 4–5  $\mu\text{m}$  thickness. The electrodes coated with the  $\text{TiO}_2$  pastes were gradually heated under airflow at 325 °C for 5 min, at 375 °C for 5 min, and at 450 °C for 15 min, and finally, kept at 500 °C for another 15 min. On the other hand, the size of the  $\text{TiO}_2$  electrodes used was 0.283  $\text{cm}^2$ . To prepare the counter electrode, two holes (1 mm diameter)

were drilled on the FTO glass by sandblasting. The perforated sheet was washed with DI water and 99.9% ethanol sequentially and cleaned ultrasound in a solution bath ( $\text{H}_2\text{O}$ : EtOH=1:1) for 5 min. After removing residual organic contaminants by heating in air for 20 min at 400 °C, Pt catalyst was deposited on the FTO glass by coating with a drop of  $\text{H}_2\text{PtCl}_6$  solution (2 mg Pt in 1 ml ethanol) with repetition of the heat treatment at 400 °C for 15 min.

#### Cell assembly

After sintering at high temperature,  $\text{TiO}_2$  was cooled down carefully to avoid glass cracks induced by sudden temperature drop. When cooling to 80 °C, the  $\text{TiO}_2$  electrode was immersed into a 0.5 mM N719 dye solution in a mixture of acetonitrile and tert-butyl alcohol (volume ratio, 1:1) and kept at room temperature for 24 h to assure complete sensitizer uptake. FTO glass coated with  $\text{H}_2\text{PtCl}_6$  was served as counter electrodes. The  $\text{TiO}_2$  electrode with N719 dye and Pt-counter electrode were assembled into a sandwich-type cell and sealed with a hot melt gasket of 60  $\mu\text{m}$  thick made of ionomer Surlyn 1702 (Dupont) at 130 °C. The electrolyte was injected into the gap between  $\text{TiO}_2$  and counter electrodes as shown below. This is a common-use method for liquid-type electrolytes which has lower viscosity. For polymer electrolytes with higher viscosity, we tried to heat it to decrease the viscosity at 70 °C and then injected to the cell in the same way.

#### Characterization and instruments

Ionic conductivities were measured by AC impedance spectroscopy using a Solatron impedance analyzer (SI-1260) and a potentiostat/galvanostat electrochemical interface (SI-1286) with a frequency range of 0.1–100 kHz, an AC amplitude of 10 mV, and a temperature range of 23–

90 °C. The specific ionic conductivity,  $\sigma$ , was obtained from  $\sigma = l/AR$ , where  $l=0.5$  cm is the distance between the two stainless steel electrodes,  $A=1$  cm<sup>2</sup> is the measured area of each electrode, and  $R$  is the measured resistance ( $\Omega$ ). The compatibility of the investigated polymer electrolytes with the stainless electrode was determined by AC impedance analysis under open-circuit conditions at different temperatures. Rheological characterizations of the polysiloxane electrolytes were done using an Advanced Rheometer AR 2000 (TA Instrument).

NMR experiments were performed using a Varian Unity INOVA 500 MHz NMR spectrometer equipped with a Chemagnetics 7.5-mm magic angle spinning probe and a double-tuned wide-line probe. The <sup>1</sup>H and <sup>13</sup>C chemical shifts are reported relative to the NMR solvent as an internal standard and the <sup>29</sup>Si chemical shifts are reported relative to an external TMS standard. NMR spectra were recorded using samples dissolved in d-solvent, CDCl<sub>3</sub>, unless otherwise stated. Photovoltaic measurements employed an AM 1.5 solar simulator equipped with a 450 W xenon lamp (model no.81172, Oriel). The power of the simulated light was calibrated to 100 mW cm<sup>-2</sup> by using a reference Si photodiode equipped with an IR-cutoff filter (KG-3, Schott) in order to reduce the mismatch between the simulated light and AM1.5 (in the region of 350–750 nm) to less than 2% with measurements verified at two solar-energy institutes [ISE (Germany), NREL (USA)]. *I-V* curves were obtained by applying an external bias (0–0.8 V) to the cell and measuring the generated photocurrent with a Keithley model 2400 digital source meter. The voltage step and delay time of photocurrent were 10 mV and 40 ms, respectively. The *I-V* curves and related characteristics of cells including open-circuit voltage ( $V_{oc}$ ), short-circuit current density ( $J_{sc}$ ), the maximum power, fill factor, and the energy conversion efficiency were automatically obtained at the same time.

## Results and discussion

The synthesis and characterization of polymer electrolytes

### Synthesis

Substituted polysiloxane electrolytes were synthesized using the hydrosilylation catalysis method. Precursors with variable -Si-H functionalities were prepared by tuning the relative ratios of PMHS and PEGMEMA as shown in Scheme 1. The light brown color and the absence of reactants in the <sup>1</sup>H, <sup>13</sup>C, <sup>29</sup>Si NMR, and FTIR analyses imply the formation of the product. The proposed mechanism, for the formation of acrylate isomers (CH<sub>3</sub>CH=CH<sub>2</sub>-OR) by the hydrosilylation reaction, involves dissociation of the PMHS ligand and subsequent gener-

ations of a solution by the Pt species [23]. This leads to hydrophilic side outgrowth and coloration of the product. Figure 1a, b shows the <sup>1</sup>H spectra of the precursor and the product, respectively. From Fig. 1a, -Si-H sensitive bonding absorbance difference of 4.85 ppm was observed from the precursor. However, the reacted functional group following the hydrosilylation reaction does not have an -Si-H group to NPSEO as shown in Fig. 1b. In addition, the EO side groups appear at 3.25–3.8 ppm as a multi-let peak in Fig. 1b, which indicates the formation of acrylate. The <sup>1</sup>H NMR spectrum did not reveal any -CH<sub>2</sub>=CH-resonance at 5.1 and 5.9 ppm, while FTIR analysis of NPSEO solid electrolyte after purification confirm the formation of these products. Also, -Si-H stretching frequency at 2,160 cm<sup>-1</sup> and -CH<sub>2</sub>=CH- frequency at 1,635 cm<sup>-1</sup> were not observed. The above data indicates that the precursors reacted completely to form the product. In addition, similar evidence appears in the <sup>29</sup>Si NMR spectrum since there is no apparent -Si-H absorbance at -34.7 ppm.

### Ionic conductivity

Figure 2 illustrates the impact of PSEO ( $n=45$ ) and NPSEO ( $n=7$ ) repeated units on ionic conductivity. The ionic conductivity increases with a decrease in the repeated units of PMHS at temperatures between 25 and 90 °C. The effect of the repeated units of PMHS on conductivity reduces as the temperature approaches  $T_g$ . Therefore, the electrolyte with a flexible backbone effectively supports the migration mechanism of ionic transport. The maximum conductivities ( $\sigma$ ) of NPSEO are  $1.0 \times 10^{-4}$  and  $1.18 \times 10^{-3}$  S cm<sup>-1</sup> at room temperature and 90 °C, respectively. The conductivity plots have the curvature characteristic of an ion transport that relies on the segmental motion of the repeat units of PMHS, and the polysiloxane backbone. Vogel-Tamman-Fulcher (VTF) equation is used to accommodate the behavior of the temperature-dependent conductivities of these electrolytes to the following parameters, namely, reflecting the number of charge carriers ( $A$ ), the apparent activation energy ( $B$ ), and the ideal glass transition temperature ( $T_0$ ). The following VTF equation [24] is used to identify the activation energy,  $E_a$ , of the ionic mobility from the assumption that the temperature dependence of  $\sigma$  demonstrates VTF behavior,

$$\sigma = AT^{-1/2} \exp(-B/R(T - T_0))$$

Figure 2 summarizes the results of ionic conductivity and activation energy of substituted polysiloxanes at various temperatures. The data reveals that NPSEO has lower number of repeat unit and the lowest activation energy of

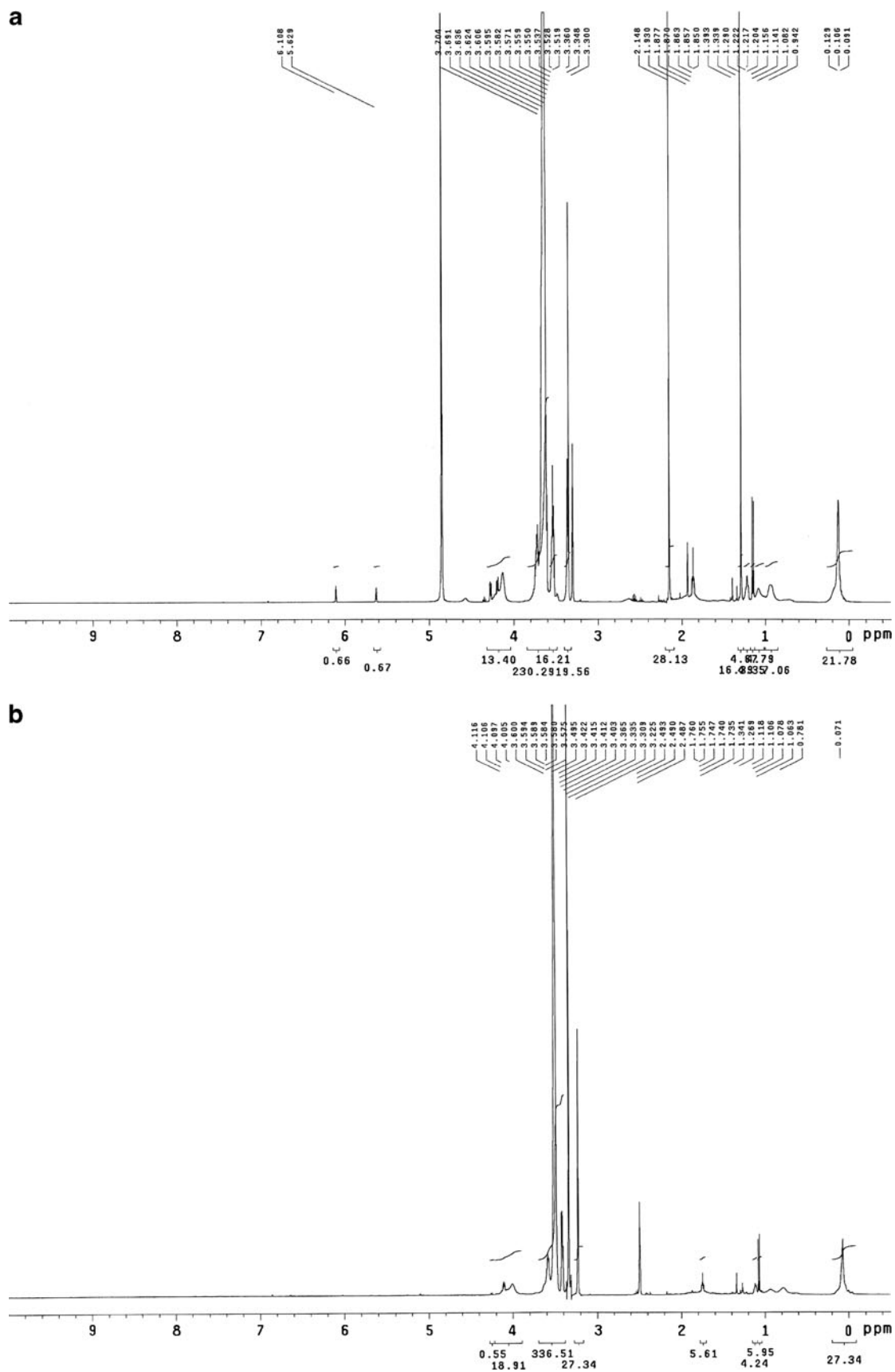
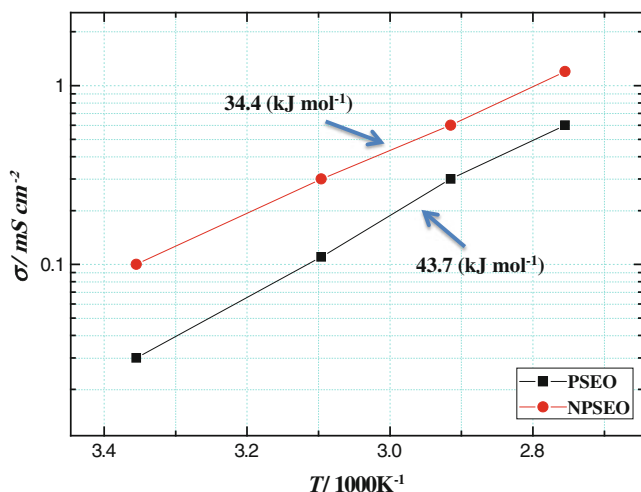


Fig. 1 Representative of <sup>1</sup>H NMR spectrum of a precursor and b NPSEO





**Fig. 2** Ionic conductivity and activation energy of substituted polysiloxanes with various temperatures

$34.4 \text{ kJ mol}^{-1}$ . Therefore, NPSEO shows higher ionic conductivity than other polysiloxane compounds at room temperature. This indicates that ionic transfer can be promoted by reducing the molecular weight of the main chain. In addition, this study can adequately illustrate the dependence of the ionic conductivity by decreasing a repeat unit of PMHS level as the result of two opposing effects. On the other hand, charge carriers from lithium iodide increase as the number of repeated units of PMHS increases. However, a decrease in the flexibility of the polymer structure eventually offsets, which impedes ion migration in the polymer electrolyte with the smallest number of main chain.

### Rheology

A Newtonian fluid has a linear stress versus strain rate curve that passes through the origin [25]. Figure 3a, b

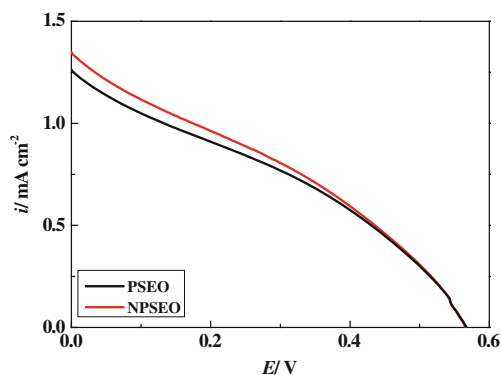


**Fig. 4**  $I$ - $V$  curves measured at AM 1.5 of DSSCs employing two polysiloxanes in the first day

shows viscosity of hydrophilic polysiloxanes PSEO and NPSEO at various temperatures, respectively, as a function of shear rate. PSEO displays a non-Newtonian fluid property because of the length of side chain which increases overall chain mobility and enhances chain packing density of the polymer with larger molecular weight. Otherwise, the side chains probably intertwine with each other and occupy free volume space of the polymer [20]. However, these phenomena provide a short route for transferring the ions since the chains are getting closer; this indicates that the PSEO offer a clear interpretation of the reduction of inter-site hopping distances and represents the ionic transfer effect as a non-Newtonian fluid electrolyte. Nevertheless, the NPSEO shows Newtonian fluid behavior as seen in Fig. 3b. In addition, this behavior becomes sensitive to temperature variation. This result can explain why the NPSEO has a lower polymer packing density and provides additional empty space for ionic transfer. Conversely, the increase in temperature enables the vibration of the side chains and the NPSEO becomes a similar fluid state. It

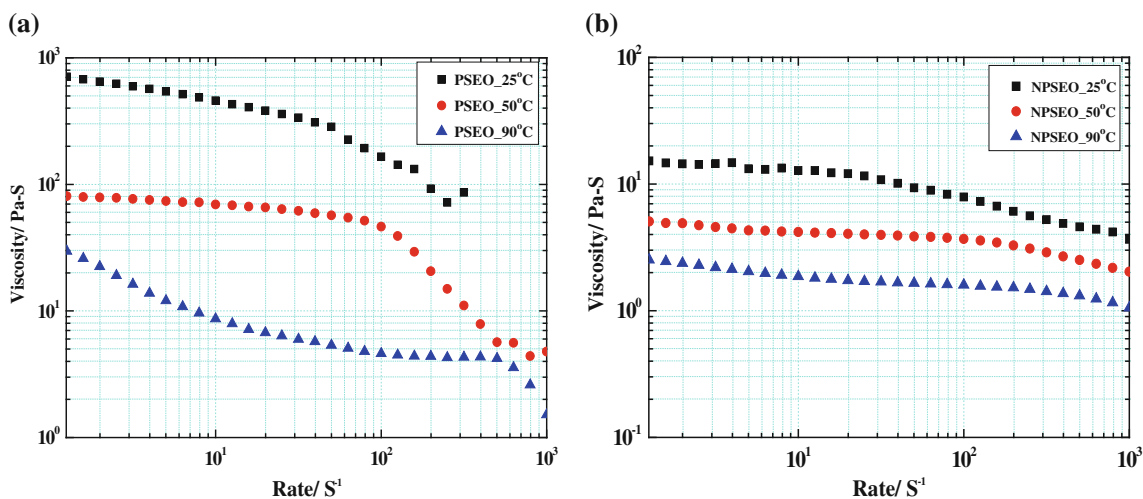


**Fig. 3** Apparent viscosity of hydrophilic polysiloxanes **a** PSEO and **b** NPSEO with various temperatures as a function of shear rate

**Table 1** Long life durable performance characteristics after 16 days of DSSCs employing electrolytes at AM1.5

	$J_{sc}/\text{mA cm}^{-2}$	$V_{oc}/\text{V}$	$ff$	$\eta/\%$
AN (1st day)	9.72	0.69	0.7	4.75
PSEO (1st day)	1.26	0.57	0.33	0.24
NPSEO (1st day)	1.35	0.57	0.33	0.25
AN (16th day)	2.34	0.72	0.62	1.05
PSEO (16th day)	1.47	0.45	0.39	0.26
NPSEO (16th day)	1.74	0.47	0.41	0.33

AN acetonitrile,  $V_{oc}$  open circuit voltage,  $J_{sc}$  short-circuit current density,  $ff$  fill factor,  $\eta$  energy conversion efficiency

produces additional free volume microvoids in the polymer electrolyte. Therefore, the increase in temperature decreases the activation energy of the polymer, which is favorable for ionic transfer. The ionic conductivity measurements confirm this data. Furthermore, the results behind the two primary factors, that control ionic transport in these substituted siloxane-based electrolytes, are the EO repeat unit of PMHS and the temperature. At room temperature, the repeat unit controls the molecular weight and the free volume for the polymer proceeds to the ionic transport effect and the Newtonian fluid property. However, at different temperatures, especially high temperatures, the ionic transport relies upon the synergy effect of the free volume of the microvoids, the polymer chain vibrations, and the repeat unit of the PMHS.

Performance and stability of solar cells assembled with the polymer electrolytes

*Photovoltaic performance*

The two-polysiloxane electrolytes remain sandwiched between the  $\text{TiO}_2$  paste and the Pt counter electrode. Figure 4 shows the recorded  $I$ - $V$  curve of the fabricated

DSSC. The initial cell performance with PSEO and NPSEO provides the  $J_{sc}$  of  $1.26$  and  $1.35 \text{ mA cm}^{-2}$ , respectively. The open-circuit voltage and efficiency of solvent free DSSCs at  $0.57$  and  $0.57 \text{ V}$ , and  $0.24\%$  and  $0.25\%$  are evaluated. The cell performance is limited to the polymer electrolyte viscosity since the viscous electrolyte cannot easily permeate into  $\text{TiO}_2$  electrode compare to AN-based liquid electrolyte. However, the viscosity effect with two polymer electrolytes, used in this work, still reveals varying performance of the  $J_{sc}$ . To study the durability, the polymer electrolytes are placed for 16 days and measured their cell performance. The initial cell performance that uses PSEO and NPSEO provides an increasing  $J_{sc}$  of  $1.47$  and  $1.74 \text{ mA cm}^{-2}$ . The open-circuit voltage and efficiency of solvent-free DSSCs are evaluated to  $0.45$  and  $0.47 \text{ V}$ , and  $0.26\%$  and  $0.33\%$  due to the electrolytes gradually contacting  $\text{TiO}_2$  and increases performance. Therefore, this experiment strongly suggests that the solvent-free DSSC requires thermal effects to enhance performance before use. To encapsulate, the cell performance is affected by viscosity,  $\text{TiO}_2$  layer thickness and the ionic conductivity, duo to the route, transportation behavior and the mechanism of ionic transfer. Additionally, these brown color polymer electrolytes probably absorb a fraction of incident light, reducing effective light absorption by the dye which brought about lower cell efficiency.

The polymer DSSCs illustrates an excellent 16 days of durable test results when compared to the AN-based liquid cell as shown in Table 1. It is easy to understand that liquid electrolytes can provide initial high efficiency, however, the evaporation of electrolyte and the leakage problems limit the practical application. In addition, the Newtonian fluid electrolyte of NPSEO provides better structural stability for ionic migration during redox reaction and lower viscosity for manufacturing. Until now, the suitable  $\text{TiO}_2$  electrode, for solvent-free polymer electrolytes, is still being modified and extensive studies are underway.

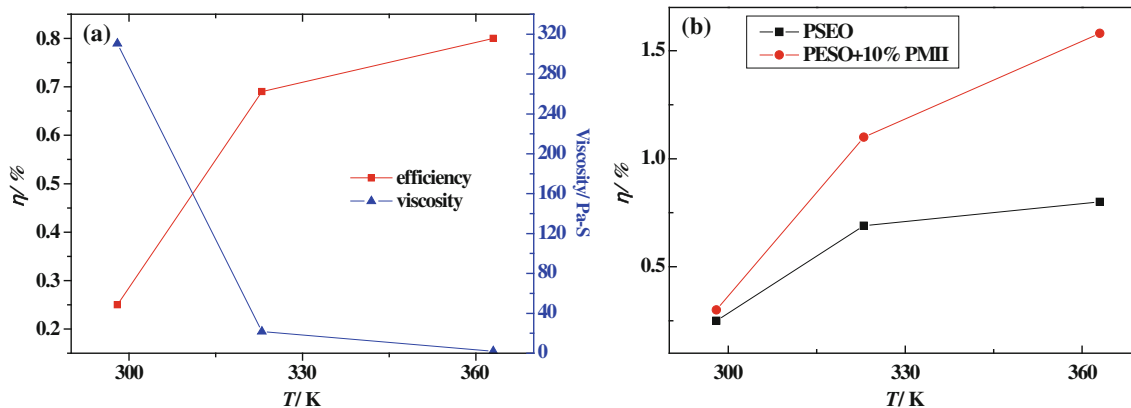


**Fig. 5** DSSC cell performances with increasing temperature employing **a** PSEO and **b** with 10% PMII addition

*Study of the effect of iodide ions and its durability under high temperatures*

Durability of the NPSEO cell performance under high temperatures is determined and shown in Fig. 5a. From this figure, it shows an energy conversion efficiency of 0.8% due to the decrease in viscosity when increasing the ionic conductivity. This explains that the polysiloxane not only has thermal stability, but also excellent recovery efficiency without a problem of crystallinity. NPSEO cell performance increases at 90 °C when the viscosity is one order lower than that the PSEO. In addition, Fig. 5b illustrates that the NPSEO mixed with 10% ionic liquid of PMII increases the iodide ion concentration of the polymer electrolyte, which enhances the amounts of redox couple and increases the efficiency of the cell to 1.5% at 90 °C. According to the literature, the primary function of DSSC is the ionic migration of the redox couple ( $I^-$  and  $I^{3-}$ ) and the solvent-free polymer electrolyte suggests a need for additional iodide ions to become a triiodide for cell reactions. From Fig. 5, an increase in efficiency (0.7%) suggests that the electrochemical redox reactions certainly improve with adequate amounts of tri-iodide and iodide ions in the electrolyte, and hence improves the DSSC performance.

## Conclusion

In this work, a novel solvent-free polysiloxane electrolyte proposed based on DSSC energy conversion efficiency. The main goal of the present work is to replace the conventional liquid type electrolyte by a nearly Newtonian fluid electrolyte which is fabricated using a repeat unit of PMHS. Substituted polysiloxane electrolytes on the FTO film has been prepared by soaking it in N719 dye to fill the vacant spaces in the  $TiO_2$  electrode. The measured open-circuit voltage and the current density of the proposed scheme using NPSEO were 0.47 V and 1.74 ( $mA\ cm^{-2}$ ), respectively, after durability test (16 days). Accordingly, the fill factor and the solar conversion efficiency were calculated as 0.41% and 0.33%. The iodide ion concentration (amounts of redox couple) increased in the polymer electrolyte after mixing with PMII and hence the efficiency of the cell increased to 1.5% at 90 °C. Furthermore, the room temperature durable test and the high temperature test of the proposed polysiloxane polymer electrolyte improved in comparison with the conventional liquid electrolyte (AN

type) DSSC. The authors of this paper expect further improvements in the conversion efficiency in their future works.

**Acknowledgment** The authors are grateful for financial support of this research from the National Science Council of Taiwan, ROC under Grant NSC 100-2923-E-011-001-MY3 and technical assistance from the Sustainable Energy Center at the National Taiwan University of Science and Technology, and the Photovoltaics Technology Center of Industrial Technology Research Institute are gratefully acknowledged.

## References

- O'Regan B, Gratzel M (1991) *Nature* 353:737
- Gratzel M (2004) *J Photochem Photobiol A Chem* 164:3
- Gorlov M, Pettersson H, Hagfeldt A, Kloo L (2007) *Inorg Chem* 46:3566
- Zhou Y, Xiang W, Chen S, Fang S, Zhou X, Zhang J, Lin Y (2009) *Electrochim Acta* 54:6645
- An SY, Jeong IC, Won MS, Jeong ED, Shim YB (2009) *J Appl Electrochem* 39:1573
- Xiao Q, Wang X, Li W, Li Z, Zhang T, Zhang H (2009) *J Membr Sci* 334:117
- Zhang J, Han H, Wu S, Xu S, Yang Y, Zhou C, Zhao X (2007) *Solid State Ionics* 178:1595
- Zhang J, Han H, Wu S, Xu S, Zhou C, Yang Y, Zhao X (2007) *Nanotechnology* 18:295606
- Tao J, Yang Y, Jin X, Qin Q (2011) *Int J Photoenergy* 2011:405738
- Akhtar MS, Kim UY, Choi DJ, Yang OB (2010) *Mater Sci Forum* 658:161
- Lin CW, Hung CL, Venkateswarlu M, Hwang BJ (2005) *J Power Sources* 146:397
- Hu L, Tang Z, Zhang Z (2007) *J Power Sources* 66:226
- Jiang G, Maeda S, Saito Y, Tanase S, Sakai T (2005) *J Electrochem Soc* 152:A767
- Croce F, Appetecchi GB, Persi L, Scrosati B (1998) *Nature* 394:456
- Watanabe M, Nishimoto A (1995) *Solid State Ionics* 79:306
- Forsyth M, MacFarlane DR, Best A, Adebahr J, Jacobsson P, Hill AJ (2002) *Solid State Ionics* 147:203
- Singh PK, Kim KW, Rhee HW (2008) *Electrochem Commun* 10:1769
- Zhang Z, Sherlock D, West R (2003) *Macromolecules* 36:9176
- Wang FM, Wan CC, Wang YY (2009) *J Appl Electrochem* 39:253
- Wang FM, Hu CC, Lo SC, Wang YY, Wan CC (2009) *Solid State Ionics* 180:405
- Wang FM, Hu CC, Lo SC, Wang YY, Wan CC (2010) *J Electroanal Chem* 644:25
- Ito S, Murakami TN, Comte P et al (2008) *Thin Solid Films* 516:4613
- Hooper R, Lyons LJ, Mapes MK (2001) *Macromolecules* 34:931
- Binesh N, Bhat S (1998) *J Polym Sci B Polym Phys* 36:1201
- Kishore N, Chhabra RP, Eswaran V (2006) *Chem Eng Res Des* 84:1180